

Original Article
Regenerative Medicine



Frozen-thawed gelatin-induced osteogenic cell sheets of canine adipose-derived mesenchymal stromal cells improved fracture healing in canine model

Yongseok Yoon , Taeseong Jung , Muhammad Afan Shahid ,
Imdad Ullah Khan , Wan Hee Kim , Oh-Kyeong Kweon *

BK21 PLUS Program for Creative Veterinary Science Research, Research Institute for Veterinary Science and College of Veterinary Medicine, Seoul National University, Seoul 08826, Korea



Received: Jul 4, 2019
Revised: Sep 3, 2019
Accepted: Sep 3, 2019

*Corresponding author:

Oh-Kyeong Kweon

Laboratory of Veterinary Surgery, College of Veterinary Medicine, Seoul National University, 1 Gwanak-ro, Gwanak-gu, Seoul 08826, Korea.
E-mail: ohkweon@snu.ac.kr

© 2019 The Korean Society of Veterinary Science

This is an Open Access article distributed under the terms of the Creative Commons Attribution Non-Commercial License (<https://creativecommons.org/licenses/by-nc/4.0>) which permits unrestricted non-commercial use, distribution, and reproduction in any medium, provided the original work is properly cited.

ORCID iDs

Yongseok Yoon 
<https://orcid.org/0000-0002-5514-447X>
Taeseong Jung 
<https://orcid.org/0000-0003-4353-8428>
Muhammad Afan Shahid 
<https://orcid.org/0000-0003-1456-6147>
Imdad Ullah Khan 
<https://orcid.org/0000-0003-2283-042X>
Wan Hee Kim 
<https://orcid.org/0000-0003-4541-2036>
Oh-Kyeong Kweon 
<https://orcid.org/0000-0003-2670-7322>

Funding

This work was carried out with the support of "Cooperative Research Program of Center

ABSTRACT

We assessed the efficacy of frozen-thawed gelatin-induced osteogenic cell sheet (FT-GCS) compared to that of fresh gelatin-induced osteogenic cell sheet (F-GCS) with adipose-derived mesenchymal stromal cells (Ad-MSCs) used as the control. The bone differentiation capacity of GCS has already been studied. On that basis, the experiment was conducted to determine ease of use of GCS in the clinic. *In vitro* evaluation of F-GCS showed 3–4 layers with an abundant extracellular matrix (ECM) formation; however, cryopreservation resulted in a reduction of FT-GCS layers to 2–3 layers. Cellular viabilities of F-GCS and FT-GCS did not vary significantly. Moreover, there was no significant difference in mRNA expressions of Runx2, β -catenin, OPN, and BMP-7 between F-GCS and FT-GCS. In an *in vivo* experiment, both legs of six dogs with transverse radial fractures were randomly assigned to one of three groups: F-GCS, FT-GCS, or control. Fracture sites were wrapped with the respective cell sheets and fixed with 2.7 mm locking plates and six screws. At 8 weeks after the operations, bone samples were collected and subjected to micro computed tomography and histopathological examination. External volumes of callus as a portion of the total bone volume in control, F-GCS, and FT-GCS groups were 49.6%, 45.3%, and 41.9%, respectively. The histopathological assessment showed that both F-GCS and FT-GCS groups exhibited significantly ($p < 0.05$) well-organized, mature bone with peripheral cartilage at the fracture site compared to that of the control group. Based on our results, we infer that the cryopreservation process did not significantly affect the osteogenic ability of gelatin-induced cell sheets.

Keywords: Gelatin-induced cell sheets; osteogenic differentiation; bone healing; dogs

INTRODUCTION

Mesenchymal stem cells can differentiate in osteocytes, adipocytes, and neurons. Therefore, they are a good source of regenerative medicine [1,2]. Injected mesenchymal stem cells can migrate to various tissues owing to their homing capacity [3]. Nevertheless, shape, size, and position of the injected stem cells are difficult to control. Recently, sheets of stem cells have

for Companion Animal Research (Project No. PJ013957)” Rural Development Administration of the Republic of Korea.

Conflict of Interest

The authors declared no conflicts of interest.

Author Contributions

Conceptualization: Kweon OK, Kim WH;
Data curation: Yoon YS, Jung TS, Shahid MA, Khan IU; Funding acquisition: Kweon OK;
Investigation: Yoon YS, Jung TS; Methodology: Yoon YS, Jung TS, Shahid MA, Khan IU; Writing - original draft: Yoon YS, Jung TS; Writing - review & editing: Shahid MA, Khan IU.

been developed to enhance cellular viability and to enhance local effects of transplanted stem cells [4]. Other *in vitro* studies have shown that osteogenic-differentiated stem cell sheet (OCSs) have osteogenic potential [5-9]. Additionally, *in vivo* application of OCSs promotes bone repair [10-13]. Previously, we have shown that gelatin-induced osteogenic cells sheets (GCSs) have improved cellular proliferation, an ample amount of extracellular matrix production, and significant upregulation of osteogenic markers compared to those of OCSs [14]. However, the *in vivo* effects of fresh and frozen-thawed gelatin-induced osteogenic cell sheets (F-GCSs and FT-GCSs, respectively) remain unclear.

Other studies have illustrated that the continuous culture of stem cells results in chromosomal aberrations and spontaneous malignant transformations [15,16]. Therefore, cryopreservation of stem cells is deemed inevitable. Moreover, at present, cryopreserved stem cells or sheets are more readily available than freshly cultured stem cells [17,18]. However, cryopreservation has its limitations as it already has been reported that cryopreservation of stem cells decreases the cells' viability, differentiation capacity, and reduces their homing ability, bio-distribution properties, and fibronectin connection capacity [19,20]. Contrary to the application of stem cells, stem cell sheets can be applied regionally to provide an improved localized effect [10,11,13]. Also, frozen-thawed OCSs can maintain their osteogenic potential and produce a highly mineralized matrix in bone defective sites [21].

Previously, we reported that GCSs are significantly better than OCSs in terms of cell proliferation, extracellular matrix (ECM) formation, and upregulation of bone markers [14]. For the present study, we hypothesized that cryopreservation not only reduces cell sheet preparation time but also do not affect the osteogenic potential of GCSs. Thus, we compared the efficacy of FT-GCSs to that of F-GCSs. In addition, we evaluated the *in vivo* bone healing capacity of both F-GCSs and FT-GCSs in a canine model.

MATERIALS AND METHODS

Isolation and culture of canine Ad-MSCs

All experiments were approved by the Institute of Animal Care and Use Committee of Seoul National University (SNU-170203-2), South Korea. In addition, all experiments were carried out in accordance with the National Institute of Health guide for the care and use of Laboratory Animals (NIH Publication No. 8023, revised 1987).

Adipose-derived mesenchymal stromal cells (Ad-MSCs) were isolated as reported previously [22]. Briefly, Ad-MSCs were isolated aseptically from gluteal adipose tissue of 2-year-old male beagle dogs. Harvested adipose tissues were washed with Dulbecco's phosphate-buffered saline (DPBS; Gibco; Fisher Scientific USA) and immersed in 1 mg/mL collagenase type I (Sigma-Aldrich, USA) at 37°C for 2 h. After treatment, the samples were washed with DPBS followed by centrifuging at 4°C and 980 × *g* for 10 min. The pellets of the stromal vascular fraction were resuspended, filtered through 100 µm nylon mesh, then incubated overnight in low-glucose Dulbecco's modified Eagle's medium (DMEM; HyClone, USA) supplemented with 10% fetal bovine serum (FBS; Gibco BRL; Fisher Scientific) and penicillin and streptomycin (PS, 10,000 U/mL, Gibco; Fisher Scientific) at 37°C in a humidified atmosphere containing 5% CO₂. After 24 h, the samples were washed with PBS to remove residual red blood and unattached cells. The medium was changed every 2 days, and the cells were sub-cultured to 90% confluence. Ad-MSCs at the third passage were used for subsequent experiments.

Preparation of fresh gelatin-induced osteogenic cells sheets (F-GCS)

F-GCSs were prepared in accordance with the method reported by Kim et al. [14]. Briefly, Ad-MSCs (5×10^5 cells) in the 3rd passage were seeded in 100 mm dishes or to 6-well plates per experimental requirements. Ad-MSCs were cultured in basal medium, low-glucose DMEM with 10% FBS (Gibco BRL; Fisher Scientific) and 1% penicillin and streptomycin (PS, 10,000 U/mL, Gibco; Fisher Scientific). When the seeded cells reached 60%–70% confluence, the basal medium was replaced with high-glucose DMEM with 10% FBS, 1% PS, 15 μ g/mL L-ascorbic acid 2-phosphate (Sigma-Aldrich, USA), 10 mM β -glycerophosphate (Sigma-Aldrich), 0.1 μ M dexamethasone (Sigma-Aldrich) and 0.02 g/mL gelatin powder (Sigma-Aldrich). The gelatin-containing differentiation medium was changed after every two days. The GCSs were harvested on the 10th day of differentiation.

Cryopreservation of GCS (FT-GCS)

Frozen-thawed GCSs (FT-GCSs) were prepared using 3rd passage GCSs and the previously described slow-freezing method [21]. After 10 days of differentiation in gelatin-containing differentiation medium, cell sheets were collected with the help of a cell scraper and transferred to 2 mL cryovials (cryogenic vial; BD Falcon). Each cryovial contained 500 μ L FBS, 400 μ L low-glucose DMEM, and 100 μ L of DMSO. Cryovials containing GCSs were cryopreserved in a freezing container (NALGENE Cryo 1°C Freezing Container; Sigma-Aldrich, USA). Container temperature was slowly decreased (1°C/min) from 4°C to -180°C. After 24 h, the samples were moved to a tank of liquid nitrogen. One week later, FT-GCSs were thawed in a water bath at 37°C. The thawed FT-GCSs were washed twice with DPBS and then used for further experimentation.

Assessment of cellular viability

Cellular viability and cell proliferation rate were calculated using a method based on assessing tetrazolium reductase activity; for that purpose, Cell counting Kit-8 was used (WST-8; Dojindo, Japan) [23,24]. We evaluated cellular viability before and after cryopreservation of the GCSs. Cell sheet samples were cultured in 1 mL of basal gelatin culture media to which 100 μ L of WST-8 solution were added. The samples were then incubated for 2 h and absorbance of the samples was measured at 450 nm. A linear relationship ($r^2 = 0.998$) between the absorbance measured and the number of diluted cells was confirmed. To determine the proliferation rate of F-GCSs and FT-GCSs, sample absorbance was measured on 0 h, 24 h, and 48 h after thawing.

Histological examination of GCS

Initially, GCSs were detached from the plates. Fixation of GCSs was carried out by using 4% paraformaldehyde and the fixed cell sheets were embedded in paraffin. Subsequently, sections (5 μ m thick) were prepared and stained with hematoxylin and eosin (H&E; Sigma-Aldrich) for histological examination.

Real-time polymerase chain reaction

Isolation of mRNA was carried out by using a Hybrid-R RNA Extraction Kit (GeneAll, Korea). Complementary DNA was prepared by using a PrimeScript II First-strand cDNA Synthesis kit (Takara, Japan). An ABI Prism 7000 Sequence Detection System (Applied Biosystems, USA) was used to amplify the desired DNA. Green Mix (Enzo Life Science, USA) was used to detect gene expressions. Normalization was done with the help of *glyceraldehyde-3-phosphate dehydrogenase* (*GAPDH*) and was quantified by using the $\Delta\Delta$ Ct method [25].

Table 1. Primers used for real-time polymerase chain reaction

Primer	Primer sequence (5'-3')	
	Forward	Reverse
GAPDH	CATTGCCCTCAATGACCACT	TCCTTGGAGGCCATGTAGAC
Runx2	TGTCATGGCGGGTAACGAT	TCCGGCCCAAAATCTCA
β -catenin	TACTGAGCCTGCCATCTGTG	ACGCAGAGGTGCATGATTG
OPN	GATGATGGAGACGATGTGGATA	TGGAATGTCAGTGGGAAAATC
BMP-7	TCGTGGAGCATGACAAAGAG	GCTCCCGAATGTAGTCCTTG

GAPDH, glyceraldehyde-3-phosphate dehydrogenase; Runx2, runt-related transcription factor 2; OPN, osteopontin; BMP-7, bone morphogenic protein 7.

All data were compared with that of fresh Ad-MSCs, which were used as the control. The primer sequences of target genes, *runt-related transcription factor 2* (*Runx2*), *β -catenin*, *osteopontin* (*OPN*), *Bone morphogenic protein 7* (*BMP-7*), and housekeeping gene *GAPDH* are shown in **Table 1**.

Capacity of mineralization

Mineralization of F-GCSs and FT-GCSs was measured on days 0, 5, and 11 of culture in gelatin-based basal media. Cell sheets were harvested and washed twice with DPBS before further processing. Afterward, cell sheets were fixed in 70% ethanol for 1 h at 25°C, followed by washing with distilled water, staining with 2% Alizarin red stain (ARS; pH 4.2), and incubation for 20 min with shaking. After aspiration of the dye, samples were washed thoroughly with distilled water, after which, 1 mL of 10 mM (10%) cetylpyridinium chloride was added and the plates incubated for 60 min with shaking. Finally, 200 μ L aliquots of the sample solution were transferred to a 96-well plate to read absorbance at 550 nm [26].

In vivo experiment

Fracture induction and cell sheet application

Six male beagle dogs, 2–3 years of age with a body weight of 8.0 ± 0.5 kg, were used in the *in vivo* study. Pre-medication of the animals was done by applying 30 mg/kg of cefazolin (Chong Kun Dang Pharmaceutical, Korea), 0.5 mg/kg famotidine (Dong-A ST, Korea), and 4 mg/kg tramadol (Samsung Pharmaceutical, Korea) before manipulation. Alfaxalone (Jurox Pty. Limited, Australia; 3 mg/kg) was used for pre-anesthetization, and intubation was carried out with an endotracheal tube. Anesthesia was maintained with isoflurane (Choongwae Pharmaceutical, Korea).

The radius bone of both right and left legs were subjected to induction of transverse fracture at the middle of the bone with an oscillation saw. The fractures were then fixed by applying a 7-hole 2.7 mm locking plate with six locking screws (BS. COREM Co., Korea). The 12 limbs of the six study dogs were randomly assigned to three groups ($n = 4$ per group): F-GCSs group, FT-GCSs group, and no treatment group (control). Three layers of respective cell sheets were applied to each limb to wrap the fracture site. Post-operative care of the dogs was carried out for seven days. All radius bones were harvested at 8 weeks after surgery for further analysis.

Radiographic and micro computed tomography examination

Radiographic examination was carried out before the operation and every week after the operation for 8 weeks. Afterward, dogs were euthanized and radius bones were harvested. The bones were then fixed with 10% neutral buffered formalin (Sigma-Aldrich, USA). The prepared bones were scanned using a micro-CT system (SKYSCAN 1172: High-Resolution Desk-top Micro-CT, Bruker, USA). Briefly, scanning was conducted using high-resolution X-ray energy settings of 85 KVP and 118 μ A with a pixel size of 31.8 μ m. Bone was considered

present at a threshold of 60-255. CTAN software (Bruker micro-CT, version 1.14.4.1; Bruker) was used to quantify bone volume and external callus amount. Using 200 layers, volume measurements were taken at 3.5 mm above and below the fracture area.

Histopathological and histomorphometric analysis

Harvested bones, at 8th week after surgery, were subjected for decalcification in 8% nitric acid and then embedded in paraffin for sectioning. Longitudinal sections were cut along a sagittal plane. Sections (4 μm thick) were used for H&E staining while 5 μm thick sections were used for Masson's trichrome staining. Stained samples were analyzed for cartilage and bone tissue formation at the fracture site. Analysis was carried out with the help of Image J (Version 1.37, National Institutes of Health, USA).

Statistical analysis

Data are presented as mean \pm standard deviation values. The IBM software SPSS Statistics 23 (SPSS Inc., USA) was used for the data analysis. Difference between groups was analyzed by applying the Kruskal-Wallis test. The Mann-Whitney U test was used as a post-hoc test. A *p* value of less than 0.05 was considered as indicative of a significant difference. *In vitro* experiments were repeated thrice.

RESULTS

Viability, histology, and proliferation of cell sheets

Number of viable cells of sheets before (F-GCSs) and after cryopreservation (FT-GCSs) were $148,130 \pm 20,880$ ($n = 16$) and $113,670 \pm 34,500$ ($n = 15$), respectively (**Fig. 1A**). There was no significant difference in number of viable cells before (F-GCSs) and after (FT-GCSs) cryopreservation. However, histological examination showed that F-GCSs were 3 to 4 layers thick while the thickness of the FT-GCSs was less, 2 to 3 layers (**Fig. 1B**). After cryopreservation, re-culturing of FT-GCSs resulted in the reduction of cellular proliferation, whereas an increasing trend was observed in F-GCSs proliferation (**Fig. 1C**). However, the decrease in the proliferation rate of re-culturing FT-GCSs, from 0 h to 48 h, was not significant (**Fig. 1C**).

Upregulation of osteogenic markers

Compared to the expression levels in Ad-MSCs, the F-GCSs and FT-GCSs both showed significant ($p < 0.05$) upregulation of *Runx2*, *β -catenin*, *OPN*, and *BMP-7*. However, there was no significant ($p > 0.05$) difference in the expressions of osteogenic genes between F-GCSs and FT-GCSs (**Fig. 2A-D**).

Degree of mineralization

Mineralization analysis showed that even after cryopreservation the FT-GCSs exhibited a significant increase in their mineralization capacity. The absorbance of ARS by F-GCSs and FT-GCSs was significantly ($p < 0.05$) higher on days 5 and 11 than on day 0 (**Fig. 3B**).

Radiographic and micro-CT imaging

Radiographic examination showed that implants retained their position for the entire 8 weeks after surgery (**Fig. 4A-I**). Groups showed no significant difference in healing at 1-week after surgery (**Fig. 4A, D, and G**). After 4 weeks of healing, all groups showed the formation of external calluses (**Fig. 4B, E, and H**), which increased in size after 8 weeks of healing (**Fig. 4C, F, and I**).

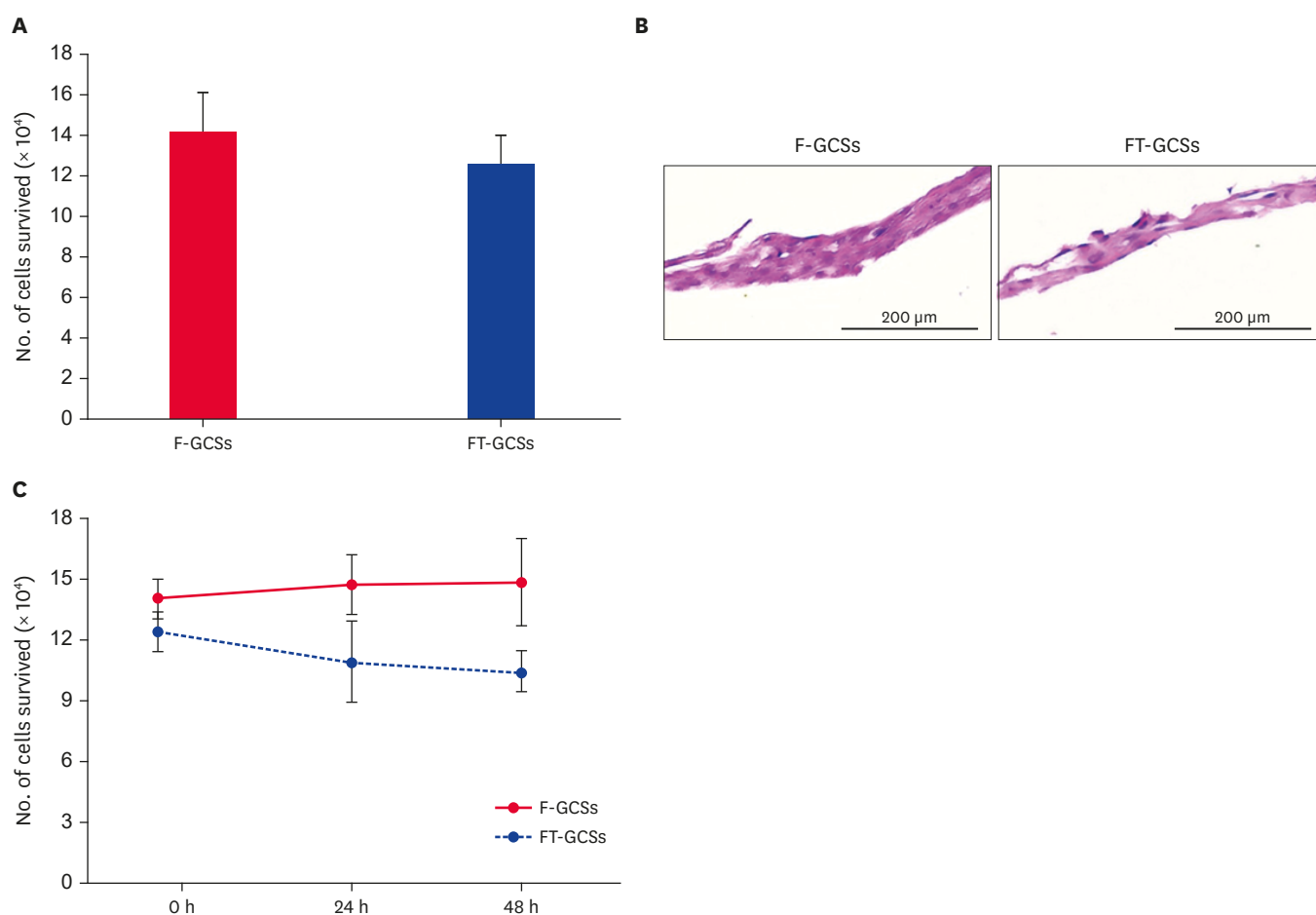


Fig. 1. Cellular viability, histology, and proliferation of F-GCSs & FT-GCSs. (A) Cellular viability of GCSs before and after cryopreservation. (B) Hematoxylin and eosin staining of cross-sections of GCSs before and after cryopreservation. Scale bars: 200 μ m. (C) There was a decrease in the cell proliferation rate of FT-GCSs, whereas F-GCSs showed an increase in proliferation. Each point represents the mean \pm standard deviation; $n = 3$.

F-GCS, fresh gelatin-induced osteogenic cell sheet; FT-GCS, frozen-thawed gelatin-induced osteogenic cell sheet; GCS, gelatin-induced osteogenic cell sheet.

Formation of large bony calluses occurred in all groups (**Fig. 4a-c**). Percentages of external callus volume out of the total bone volume for the control, F-GCSs, and FT-GCSs groups were $49.6\% \pm 1.05$, $45.3\% \pm 4.08$, and $41.9\% \pm 3.50$, respectively. There was no significant difference in callus size among the groups (**Fig. 4d**). The percentages of connectivity of cortices in each group were 21% in control, 81% in F-GCSs, and 80% in FT-GCSs ($p > 0.05$, **Fig. 4e**).

Histopathology of the fracture area

Histopathological analysis of harvested bones that were treated with F-GCSs and FT-GCSs revealed the presence of organized and mature bone with less peripheral cartilage on the fracture sites at 8 weeks after surgery (**Fig. 5D-I**). However, there was formation of cartilage with little ossification at the fracture site in the control group limbs (**Fig. 5A-C**).

Bone histomorphometric analysis of the groups treated with F-GCSs and FT-GCSs revealed significantly ($p < 0.05$) greater presences of mature bone compared to that in the control group (**Fig. 5K**). Moreover, the percentage of cartilage formation in the control group was significantly ($p < 0.05$) higher than those in the F-GCSs and FT-GCSs groups (**Fig. 5J**).

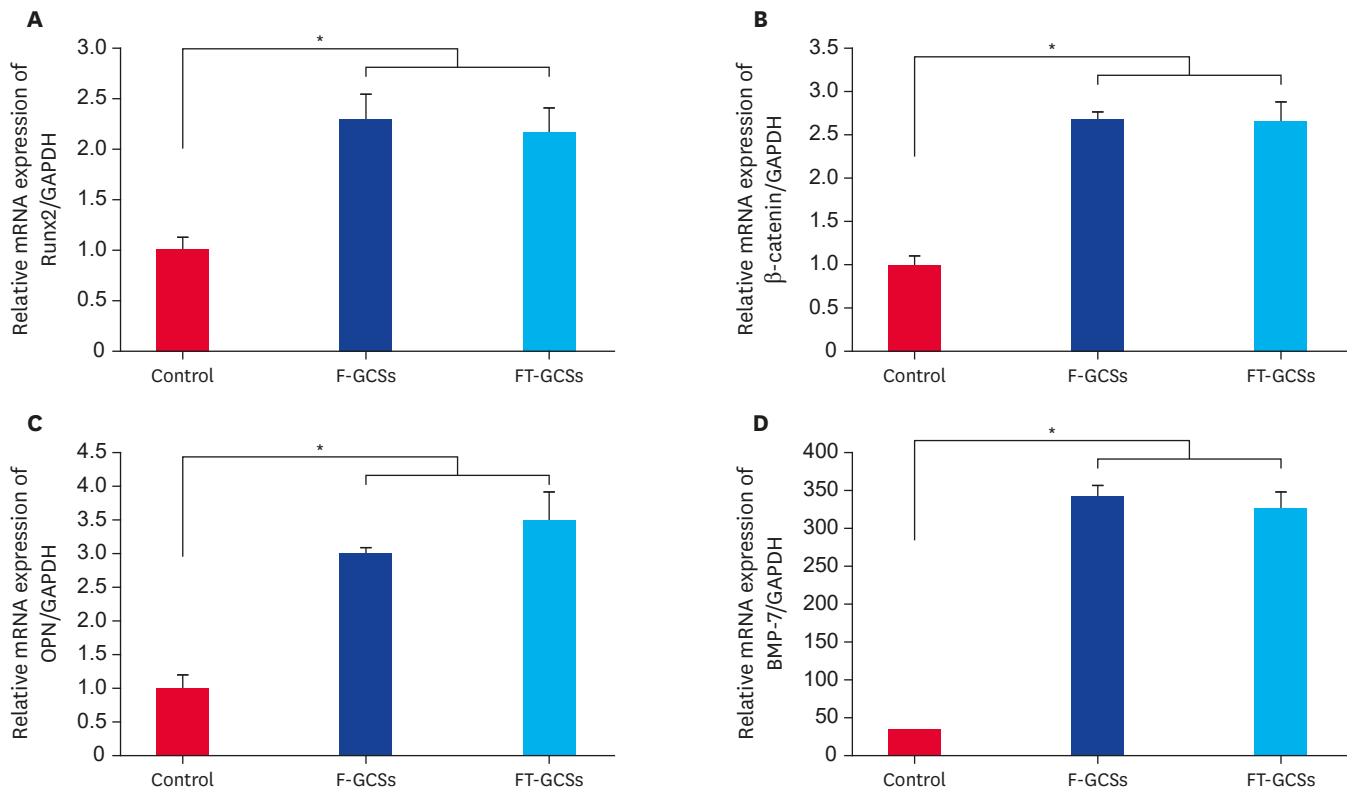


Fig. 2. Expression of osteogenic makers of adipose-derived mesenchymal stromal cells (in red), F-GCSs (in dark blue) and FT-GCSs (in blue). The mRNA expressions are relative to that of GAPDH and were evaluated by using quantitative real-time PCR for (A) Runx2, (B) β -catenin, (C) OPN, and (D) BMP-7. Each bar indicates mean \pm standard deviation; n = 3.

Runx2, runt-related transcription factor 2; GAPDH, glyceraldehyde 3-phosphate dehydrogenase; F-GCS, fresh gelatin-induced osteogenic cell sheet; FT-GCS, frozen-thawed gelatin-induced osteogenic cell sheet; OPN, osteopontin; BMP-7, bone morphogenetic protein 7.

* $p < 0.05$, significant difference from the control.

DISCUSSION

Currently, performing bone reconstruction with tissue-engineered bone or an osteogenic cell sheet (OCS) is a lengthy procedure, which involves cell isolation, seeding, culturing, differentiation, and scaffold construction [10,27]. Therefore, bone fracture surgeries must be planned to coincide with cell preparation time. Hence, protocols for cell sheet or scaffold preparation may not be convenient for clinical therapies. Clinically, there is a need for a method which can reduce cell preparation time and increase the osteogenic potential of cells. Previously, we reported that the use of F-GCSs was significantly better in terms of proliferation, ECM production, and osteogenic bone marker production than those of OCSs [14]. However, F-GCSs also need preparation before administration, which can delay treatment of a bone fracture. Consequently, FT-GCSs was a suggested solution to that problem, as it showed good potential for mineralization and mature bone production. In addition, the immediate application of thawed FT-GCSs made its use more desirable and convenient than the use of F-GCSs or fresh-OCSs when supporting the healing of fractured bones.

This study revealed that FT-GCSs maintain the structural integrity of F-GCSs, and FT-GCSs produce extensive mineralization even after thawing. Although the number of viable cells and the thickness of the layers were lower in the FT-GCSs group than in the F-GCSs group, the differences were not significant. Thawing resulted in a decrease of cellular viability of FT-GCSs

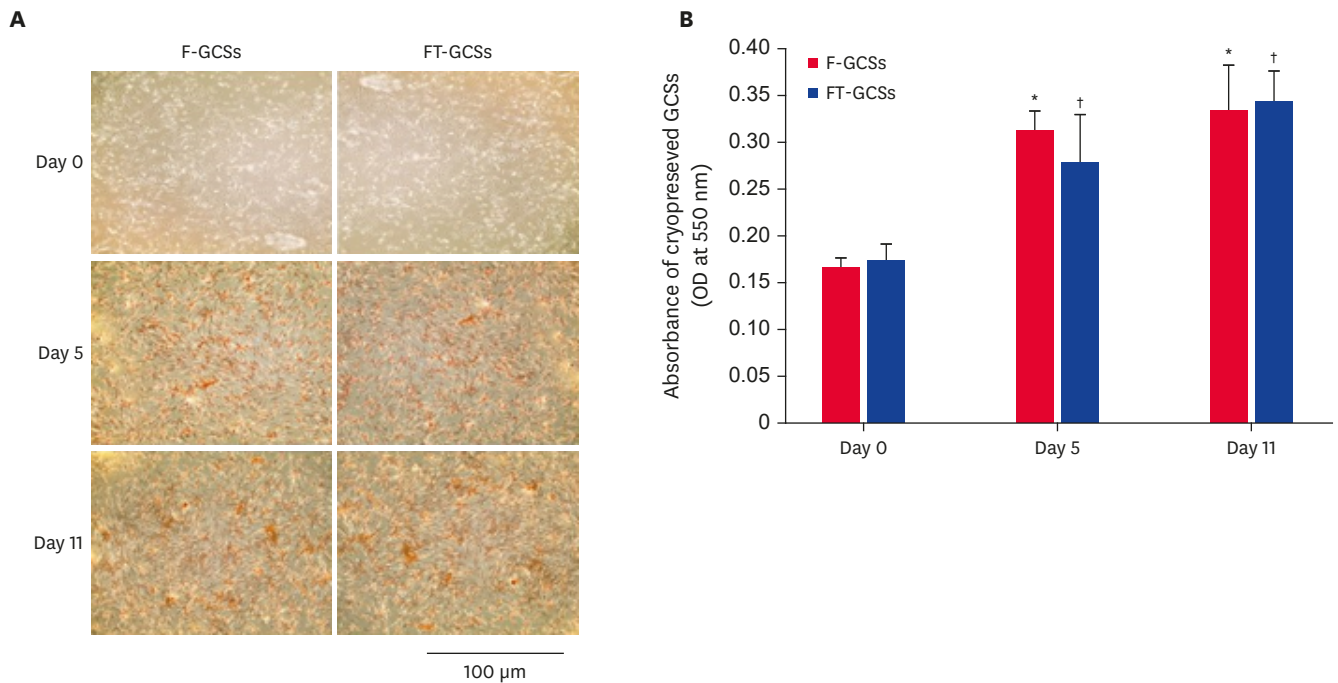


Fig. 3. Mineralization of F-GCSs and FT-GCSs. (A) Alizarin red staining of F-GCSs and FT-GCSs after 0, 5, and 11 days of culture (Scale bar 100 μ m). (B) Absorption (at 550 nm) was observed to determine the degree of mineralization on days 0, 5, and 11 in both groups.

F-GCS, fresh gelatin-induced osteogenic cell sheet; FT-GCS, frozen-thawed gelatin-induced osteogenic cell sheet; GCS, gelatin-induced osteogenic cell sheet; OD, optical density.

* † $p < 0.05$, significant differences in F-GCSs and FT-GCSs, respectively, from that at day 0 ($n = 3$).

(*i.e.*, 76% viability compared to that of F-GCSs), which is comparable to the decrease in viability of cryopreserved OCSs (*i.e.*, 70% viability compared to fresh-OCSs), as previously reported [21]. In this study, cryopreservation was carried out for only a short period (one week); further experiments are required to evaluate the effects of longer term cryopreservation.

Previously, it was reported that F-GCSs showed significantly higher cell proliferation rate compared to that of fresh-OCS, a difference that may be due to the activation of *Wnt* [14]. In contrast, in the present study, FT-GCSs showed a downward trend in proliferation. Our results indicate that cryopreservation may have a down-regulatory effect on the *Wnt* pathway. Activation of such pathways promotes the proliferation and differentiation MSCs [28,29]. However, β -catenin expression of GCSs, reported to be an important factor within the canonical *Wnt*/ β -catenin pathway [30,31], did not differ significantly before and after cryopreservation. Moreover, there was no significant decrease in differentiation potential of FT-GCSs, indicating that some other pathway was involved in decreasing the proliferation of FT-GCSs. Further experiments are required in order to explain the proliferation decrease.

Some authors have reported that cryopreservation of MSCs does not affect their osteogenic differentiation [32]. However, dimethyl sulfoxide (DMSO) is reported to have cytotoxic effects and induces differentiation of MSCs into neuron-like cells [33] or cardiac myocytes [34]. Our study results, showing no significant difference in the osteogenic differentiation and mineralization of FT-GCSs as compared to F-GCSs, support those studies that have reported that cryopreservation of stem cells sheets with DMSO does not alter mineralization or bone production capacity [24].

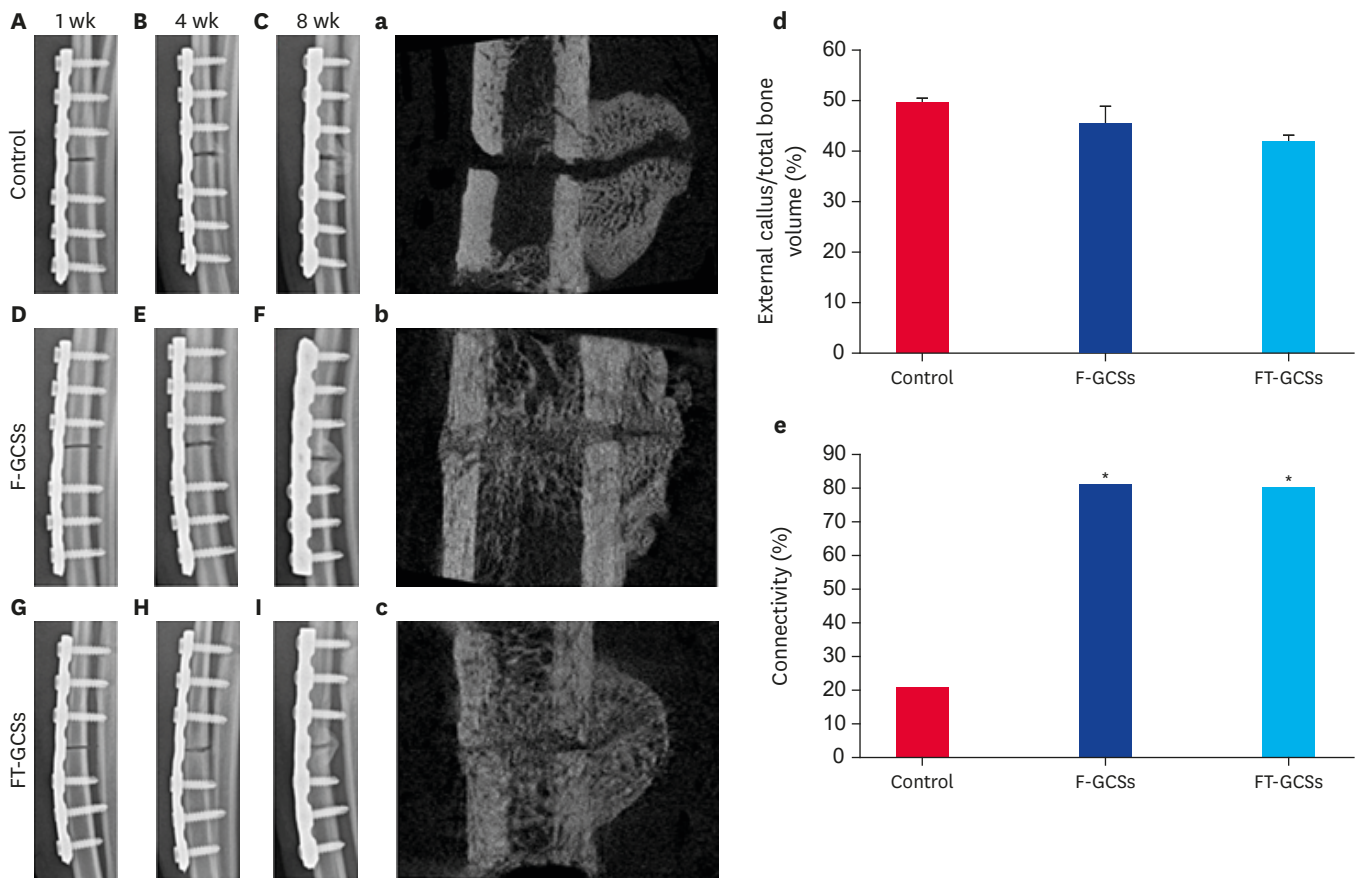


Fig. 4. Radiographic & micro-computed tomography images. (A-I) Radiographic examination showed that implants retained their position for the entire 8 weeks after surgery. (a-c) All groups showed the formation of large bony calluses but different percentages of bone connectivity. (d) There were no significant differences in the proportion of callus out of the total bone volume among the groups. (e) F-GCSs and FT-GCSs showed significantly better cortical bone connectivity than that of the control after 8 weeks of surgery.

FT-GCS, frozen-thawed gelatin-induced osteogenic cell sheet; F-GCS, fresh gelatin-induced osteogenic cell sheet.

* $p < 0.05$, significant difference from the control ($n = 4$).

These results were also supported by our real-time PCR results, which showed that expression levels of *Runx2*, *OPN*, and *BMP-7* of FT-GCSs remained almost equal to those of F-GCSs. *Runx2* is an important indicator of early osteogenic differentiation, while *OPN* and *BMP-7* are produced from mature osteoblasts in later stages of osteogenesis [35,36]. Therefore, the results indicate GCSs differentiate into mature osteoblasts, and neither freezing-thawing nor DMSO has a significant negative effect on the osteogenic differentiation capacity of GCSs. Alizarin red stain (ARS) results showed that mineralization of FT-GCSs was significantly increased in the 5th and 11th day as compared to that on the 0th day of reculturing, suggesting that the osteogenic differentiation process, which was suspended as a result of cryopreservation, proceed continuously after thawing.

Various studies have reported the formation of a callus at the fracture site, even in the presence of strict fixation [10,37,38]. In this study, callus formation was observed in the control, F-GCSs, and FT-GCSs groups. This could be the result of secondary healing of the bones. Micro-motions and periosteal reaction could also have an effect on callus formation in all groups. Regardless, the F-GCSs and FT-GCSs groups had better healing capacities than the control group. Despite the same nature of fixation as that applied in the control group, there was a more formation of mature bone in F-GCSs and FT-GCSs groups. In addition,

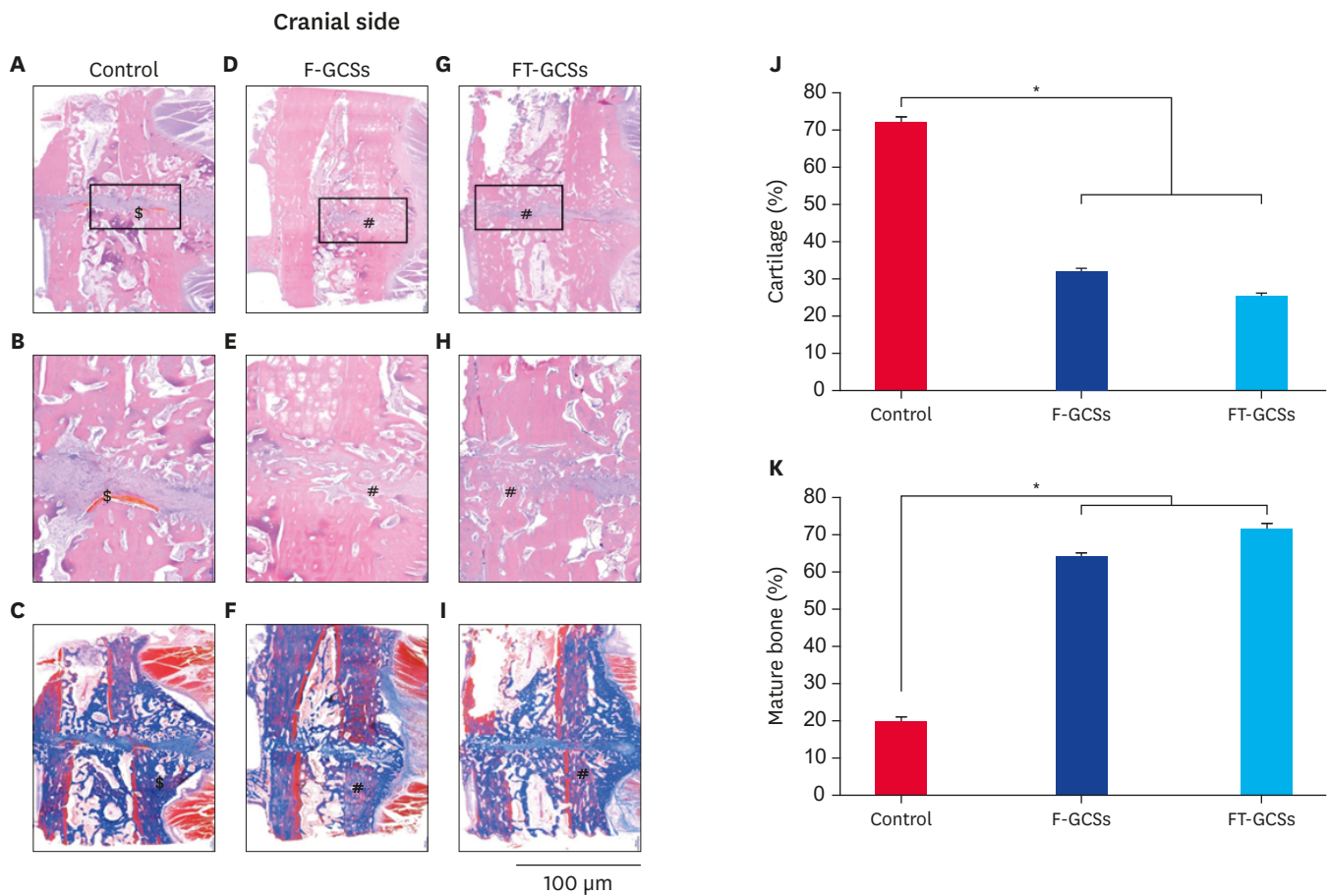


Fig. 5. Histopathological staining of longitudinal sections of radius bone with mid-shaft transverse fracture after 8 weeks of healing with decalcification. (A-C) Control group showed cartilage formation (\$) without ossification at the fracture site. (D-I) F-GCSs and FT-GCSs groups showed fracture sites were well-organized with both cartilage and mature bone (#) present. (B, E, H) are magnified images of A, D, and G, respectively. (J) The control treatment produced a significant ($p < 0.05$) presence of cartilage rather than mature bone (K); however, F-GCSs and FT-GCSs produced a significant ($p < 0.05$) presence of mature bone at the healing sites compared to that in the control.

F-GCS, fresh gelatin-induced osteogenic cell sheet; FT-GCS, frozen-thawed gelatin-induced osteogenic cell sheet.

* $p < 0.05$, significant difference from the control (Scale bar: 100 μ m; n = 4).

there was no significant difference in *BMP-7* expression between FT-GCSs and F-GCSs, which might be involved in the high level of mature bone production, less connective tissue formation, and fast healing time of fractures in the F-GCSs and FT-GCSs groups [36,39].

Injected stem cells can resettle to a specific tissue owing to their homing characteristics [3] However, cryopreservation has been reported to have a negative effect on homing characteristics of stem cells [19], reducing the homing ability of stem cells. However, cell sheets can be used in a localized area, therefore, cell sheets can be used more efficiently than stem cells [21]. Moreover, gelatin contains an arginine-glycine-aspartic acid (RGD) sequence, which promotes cells stability with ECM [40] and cell adhesion through integrin [41,42].

It is concluded that freezing and thawing did not affect the osteogenic ability of GCSs. Moreover, FT-GCSs can be utilized immediately after thawing with the same effects as those produced by F-GCSs.

Therefore, compared to F-GCSs, the use of FT-GCSs for fracture healing is more convenient.

REFERENCES

1. Parekkadan B, Milwid JM. Mesenchymal stem cells as therapeutics. *Annu Rev Biomed Eng* 2010;12:87-117. [PUBMED](#) | [CROSSREF](#)
2. Uccelli A, Moretta L, Pistoia V. Mesenchymal stem cells in health and disease. *Nat Rev Immunol* 2008;8:726-736. [PUBMED](#) | [CROSSREF](#)
3. Devine SM, Cobbs C, Jennings M, Bartholomew A, Hoffman R. Mesenchymal stem cells distribute to a wide range of tissues following systemic infusion into nonhuman primates. *Blood* 2003;101:2999-3001. [PUBMED](#) | [CROSSREF](#)
4. Kelm JM, Fussenegger M. Scaffold-free cell delivery for use in regenerative medicine. *Adv Drug Deliv Rev* 2010;62:753-764. [PUBMED](#) | [CROSSREF](#)
5. Akahane M, Nakamura A, Ohgushi H, Shigematsu H, Dohi Y, Takakura Y. Osteogenic matrix sheet-cell transplantation using osteoblastic cell sheet resulted in bone formation without scaffold at an ectopic site. *J Tissue Eng Regen Med* 2008;2:196-201. [PUBMED](#) | [CROSSREF](#)
6. Guo P, Zeng JJ, Zhou N. A novel experimental study on the fabrication and biological characteristics of canine bone marrow mesenchymal stem cells sheet using vitamin C. *Scanning* 2015;37:42-48. [PUBMED](#) | [CROSSREF](#)
7. Ma D, Ren L, Liu Y, Chen F, Zhang J, Xue Z, Mao T. Engineering scaffold-free bone tissue using bone marrow stromal cell sheets. *J Orthop Res* 2010;28:697-702. [PUBMED](#)
8. Wei F, Qu C, Song T, Ding G, Fan Z, Liu D, Liu Y, Zhang C, Shi S, Wang S. Vitamin C treatment promotes mesenchymal stem cell sheet formation and tissue regeneration by elevating telomerase activity. *J Cell Physiol* 2012;227:3216-3224. [PUBMED](#) | [CROSSREF](#)
9. Kuk M, Kim Y, Lee SH, Kim WH, Kweon OK. Osteogenic ability of canine adipose-derived mesenchymal stromal cell sheets in relation to culture time. *Cell Transplant* 2016;25:1415-1422. [PUBMED](#) | [CROSSREF](#)
10. Yoon Y, Khan IU, Choi KU, Jung T, Jo K, Lee SH, Kim WH, Kim DY, Kweon OK. Different bone healing effects of undifferentiated and osteogenic differentiated mesenchymal stromal cell sheets in canine radial fracture model. *Tissue Eng Regen Med* 2017;15:115-124. [PUBMED](#) | [CROSSREF](#)
11. Inagaki Y, Uematsu K, Akahane M, Morita Y, Ogawa M, Ueha T, Shimizu T, Kura T, Kawate K, Tanaka Y. Osteogenic matrix cell sheet transplantation enhances early tendon graft to bone tunnel healing in rabbits. *BioMed Res Int* 2013;2013:842192. [PUBMED](#) | [CROSSREF](#)
12. Pirraco RP, Obokata H, Iwata T, Marques AP, Tsuneda S, Yamato M, Reis RL, Okano T. Development of osteogenic cell sheets for bone tissue engineering applications. *Tissue Eng Part A* 2011;17:1507-1515. [PUBMED](#) | [CROSSREF](#)
13. Uchiyama H, Yamato M, Sasaki R, Sekine H, Yang J, Ogiuchi H, Ando T, Okano T. *In vivo* 3D analysis with micro-computed tomography of rat calvaria bone regeneration using periosteal cell sheets fabricated on temperature-responsive culture dishes. *J Tissue Eng Regen Med* 2011;5:483-490. [PUBMED](#) | [CROSSREF](#)
14. Kim AY, Kim Y, Lee SH, Yoon Y, Kim WH, Kweon OK. Effect of gelatin on osteogenic cell sheet formation using canine adipose-derived mesenchymal stem cells. *Cell Transplant* 2017;26:115-123. [PUBMED](#) | [CROSSREF](#)
15. Froelich K, Mickler J, Steusloff G, Technau A, Ramos Tirado M, Scherzed A, Hackenberg S, Radeloff A, Hagen R, Kleinsasser N. Chromosomal aberrations and deoxyribonucleic acid single-strand breaks in adipose-derived stem cells during long-term expansion *in vitro*. *Cytotherapy* 2013;15:767-781. [PUBMED](#) | [CROSSREF](#)
16. Roemeling-van Rhijn M, de Klein A, Douben H, Pan Q, van der Laan LJ, Ijzermans JN, Betjes MG, Baan CC, Weimar W, Hoogduijn MJ. Culture expansion induces non-tumorigenic aneuploidy in adipose tissue-derived mesenchymal stromal cells. *Cytotherapy* 2013;15:1352-1361. [PUBMED](#) | [CROSSREF](#)
17. Bruder SP, Jaiswal N, Haynesworth SE. Growth kinetics, self-renewal, and the osteogenic potential of purified human mesenchymal stem cells during extensive subcultivation and following cryopreservation. *J Cell Biochem* 1997;64:278-294. [PUBMED](#) | [CROSSREF](#)

18. Spurr EE, Wiggins NE, Marsden KA, Lowenthal RM, Ragg SJ. Cryopreserved human haematopoietic stem cells retain engraftment potential after extended (5–14 years) cryostorage. *Cryobiology* 2002;44:210-217.
[PUBMED](#) | [CROSSREF](#)
19. Chinnadurai R, Garcia MA, Sakurai Y, Lam WA, Kirk AD, Galipeau J, Copland IB. Actin cytoskeletal disruption following cryopreservation alters the biodistribution of human mesenchymal stromal cells *in vivo*. *Stem Cell Reports* 2014;3:60-72.
[PUBMED](#) | [CROSSREF](#)
20. Pal R, Hanwate M, Totev SM. Effect of holding time, temperature and different parenteral solutions on viability and functionality of adult bone marrow-derived mesenchymal stem cells before transplantation. *J Tissue Eng Regen Med* 2008;2:436-444.
[PUBMED](#) | [CROSSREF](#)
21. Kura T, Akahane M, Shimizu T, Uchihara Y, Tohma Y, Morita Y, Koizumi M, Kawate K, Tanaka Y. Use of cryopreserved osteogenic matrix cell sheets for bone reconstruction. *Stem Cell Discovery* 2016;06:13-23.
[CROSSREF](#)
22. Ryu HH, Lim JH, Byeon YE, Park JR, Seo MS, Lee YW, Kim WH, Kang KS, Kweon OK. Functional recovery and neural differentiation after transplantation of allogenic adipose-derived stem cells in a canine model of acute spinal cord injury. *J Vet Sci* 2009;10:273-284.
[PUBMED](#) | [CROSSREF](#)
23. Kito K, Kagami H, Kobayashi C, Ueda M, Terasaki H. Effects of cryopreservation on histology and viability of cultured corneal epithelial cell sheets in rabbit. *Cornea* 2005;24:735-741.
[PUBMED](#) | [CROSSREF](#)
24. Shimizu T, Akahane M, Ueha T, Kido A, Omokawa S, Kobata Y, Murata K, Kawate K, Tanaka Y. Osteogenesis of cryopreserved osteogenic matrix cell sheets. *Cryobiology* 2013;66:326-332.
[PUBMED](#) | [CROSSREF](#)
25. Livak KJ, Schmittgen TD. Analysis of relative gene expression data using real-time quantitative PCR and the 2⁻(Delta Delta C(T)) Method. *Methods* 2001;25:402-408.
[PUBMED](#) | [CROSSREF](#)
26. Gregory CA, Gunn WG, Peister A, Prockop DJ. An Alizarin red-based assay of mineralization by adherent cells in culture: comparison with cetylpyridinium chloride extraction. *Anal Biochem* 2004;329:77-84.
[PUBMED](#) | [CROSSREF](#)
27. Okamoto M, Dohi Y, Ohgushi H, Shimaoka H, Ikeuchi M, Matsushima A, Yonemasu K, Hosoi H. Influence of the porosity of hydroxyapatite ceramics on *in vitro* and *in vivo* bone formation by cultured rat bone marrow stromal cells. *J Mater Sci Mater Med* 2006;17:327-336.
[PUBMED](#) | [CROSSREF](#)
28. Dravid G, Ye Z, Hammond H, Chen G, Pyle A, Donovan P, Yu X, Cheng L. Defining the role of Wnt/beta-catenin signaling in the survival, proliferation, and self-renewal of human embryonic stem cells. *Stem Cells* 2005;23:1489-1501.
[PUBMED](#) | [CROSSREF](#)
29. Gaur T, Lengner CJ, Hovhannisyan H, Bhat RA, Bodine PV, Komm BS, Javed A, van Wijnen AJ, Stein JL, Stein GS, Lian JB. Canonical WNT signaling promotes osteogenesis by directly stimulating Runx2 gene expression. *J Biol Chem* 2005;280:33132-33140.
[PUBMED](#) | [CROSSREF](#)
30. Zhang JF, Li G, Chan CY, Meng CL, Lin MC, Chen YC, He ML, Leung PC, Kung HF. Flavonoids of *Herba Epimedii* regulate osteogenesis of human mesenchymal stem cells through BMP and Wnt/beta-catenin signaling pathway. *Mol Cell Endocrinol* 2010;314:70-74.
[PUBMED](#) | [CROSSREF](#)
31. Macsai CE, Foster BK, Xian CJ. Roles of Wnt signalling in bone growth, remodelling, skeletal disorders and fracture repair. *J Cell Physiol* 2008;215:578-587.
[PUBMED](#) | [CROSSREF](#)
32. Kotobuki N, Hirose M, Machida H, Katou Y, Muraki K, Takakura Y, Ohgushi H. Viability and osteogenic potential of cryopreserved human bone marrow-derived mesenchymal cells. *Tissue Eng* 2005;11:663-673.
[PUBMED](#) | [CROSSREF](#)
33. Chu Q, Wang Y, Fu X, Zhang S. Mechanism of *in vitro* differentiation of bone marrow stromal cells into neuron-like cells. *J Huazhong Univ Sci Technol Med Sci* 2004;24:259-261.
[PUBMED](#) | [CROSSREF](#)
34. Young DA, Gavrillov S, Pennington CJ, Nuttall RK, Edwards DR, Kitsis RN, Clark IM. Expression of metalloproteinases and inhibitors in the differentiation of P19CL6 cells into cardiac myocytes. *Biochem Biophys Res Commun* 2004;322:759-765.
[PUBMED](#) | [CROSSREF](#)

35. Chen G, Deng C, Li YP. TGF- β and BMP signaling in osteoblast differentiation and bone formation. *Int J Biol Sci* 2012;8:272-288.
[PUBMED](#) | [CROSSREF](#)
36. Komori T. Regulation of skeletal development by the Runx family of transcription factors. *J Cell Biochem* 2005;95:445-453.
[PUBMED](#) | [CROSSREF](#)
37. Nakamura A, Akahane M, Shigematsu H, Tadokoro M, Morita Y, Ohgushi H, Dohi Y, Imamura T, Tanaka Y. Cell sheet transplantation of cultured mesenchymal stem cells enhances bone formation in a rat nonunion model. *Bone* 2010;46:418-424.
[PUBMED](#) | [CROSSREF](#)
38. Shimizu T, Akahane M, Morita Y, Omokawa S, Nakano K, Kira T, Onishi T, Inagaki Y, Okuda A, Kawate K, Tanaka Y. The regeneration and augmentation of bone with injectable osteogenic cell sheet in a rat critical fracture healing model. *Injury* 2015;46:1457-1464.
[PUBMED](#) | [CROSSREF](#)
39. Komori T. Regulation of osteoblast differentiation by transcription factors. *J Cell Biochem* 2006;99:1233-1239.
[PUBMED](#) | [CROSSREF](#)
40. Hoch E, Schuh C, Hirth T, Tovar GE, Borchers K. Stiff gelatin hydrogels can be photo-chemically synthesized from low viscous gelatin solutions using molecularly functionalized gelatin with a high degree of methacrylation. *J Mater Sci Mater Med* 2012;23:2607-2617.
[PUBMED](#) | [CROSSREF](#)
41. Rosellini E, Cristallini C, Barbani N, Vozzi G, Giusti P. Preparation and characterization of alginate/gelatin blend films for cardiac tissue engineering. *J Biomed Mater Res A* 2009;91:447-453.
[PUBMED](#) | [CROSSREF](#)
42. Wu SC, Chang WH, Dong GC, Chen KY, Chen YS, Yao CH. Cell adhesion and proliferation enhancement by gelatin nanofiber scaffolds. *J Bioact Compat Polym* 2011;26:565-577.
[CROSSREF](#)